



Locating Underground Water Pipe Leakages Via Interpretation of Ground Penetrating Radar Signals

S.F. Senin^{1,2}, M.S. Jaafar², R.Hamid^{2*}

¹Faculty of Civil Engineering,
Universiti Teknologi MARA
Pulau Pinang, 13500 Permatang Pauh, Penang, Malaysia
²Smart and Sustainable Township Research Centre,
Faculty of Engineering and Built Environment,
Universiti Kebangsaan Malaysia,
43600, Bangi, Selangor, Malaysia

*Corresponding author E-mail: roszilah@ukm.edu.my

Abstract

Water wastage due to leakages in the water distribution system is a common problem encountered worldwide. The detection and localization of water pipes' leakages in the underground pipe system is possible by the high-resolution images of Ground Penetrating Radar (GPR) with 1.6 GHz antenna. Experimental simulation of water leakage for shallow buried PVC pipe at a depth of 0.24 m and 0.23 m in mediums of dry sand and loose soil, respectively was performed. Holes were drilled in the middle of the pipe to allow water to leak inside the soils. The presence of water in the soils is detected as the soils' moistures influence the GPR signal reflection characteristics. The GPR images show appearance of delayed hyperbolas and the attenuation of reflection when the water content increased. The increased in dielectric constant and the reduction of wave velocity of the GPR signals in soil enabled the inspector to detect the water leakage in pipes. Results showed that the depth of the water leakages in the pipes were detected at 0.242 m 0.220 m respectively. GPR method is able to locate the underground water pipes leakages in the underground pipes accurately.

Keywords: dielectric; ground penetrating radar; soil; water leakages

1. Introduction

The percentage of water leakage loss that occurred through underground water pipes is very crucial to be considered by the local authorities and consumers, especially at the water supply and usage stage. It was estimated that approximately 20 to 30% of water loss of the total water withdrawals has been observed by The International Water Supply Association (IWSA) [1]. In Malaysia, National Water Services Commission reported that approximately 52.1% of the treated water were lost either by water leakages, damaged pipes or water theft [2]. This scenario is a worrying situation to the consumers and the local water providers as they have to bear huge financial losses every year. There is a need for non-destructive technique (NDT) which can locate buried water pipes' leakages for maintenance purpose so that water loss due to leaking pipes can be overcome.

A popular method, Ground Penetrating Radar (GPR), is a rapid and effective non-destructive method in detecting the underground pipe water leakages locations. Leakages in buried water pipe can be characterized either by detecting the underground voids as a result from water leaks caused by corrosion on the circumference of the pipe, or by detecting the changes on the dielectric constant of soil around the pipe that is caused by water saturation [3]. This method also has advantages over other methods as it offers high probability in detecting plastic pipe water leakages locations [4]. The location of water pipes leakages in soil can also be determined by detecting the changes of GPR energy that is attenuated as the reflected radar signal travels through the saturated surrounding soils created by the leaking water [5]. Detection of possible water leaks using the appearance of hyperbola or changes of GPR hyperbola geometry has also been studied [6]. They [6] extracted the hyperbola patterns and correlate them with the water leaks in order to avoid misinterpretation in leaks detection. Despite of its success in detecting water leakage location, this method is limited to detect the pipe leakages depth location not more than the maximum GPR penetration depth; depending on the GPR central frequency. Highly conductive soils containing chloride or ferric will significantly absorb and scatter the incoming GPR signal and create difficulties in locating the underground pipe.

Principally, GPR uses the electromagnetic wave transmission and reflection signals in detecting embedded pipes or utilities. The GPR transmitter antenna transmits electromagnetic wave that propagates through the soil with certain velocity, v . As the wave propagates through the soil with different dielectric constant due to the changes in moisture content from the water leakages, the velocity, v , is also greatly influenced as it is related to the medium dielectric constant, ϵ , by Equation 1 [7]:

$$v = \frac{c}{\sqrt{\epsilon}} \quad (1)$$



where c is the speed of light in vacuum, which is equals to 0.3 m/ns and ϵ is the dielectric constant of the medium.

The GPR electromagnetic wave is then reflected to the GPR receiver antenna as this wave impinge on medium of different dielectric constant due to the varying dielectric constant values [8]. For instance, the dielectric constant of aqueous solution varies between 40 (high salinity) and 81 (pure water). In sandy soil, the dielectric constants are reported to be in range of 3 to 14 [9], depending mainly on the amount of the leaking water content inside the soil and the GPR frequency.

The reflection and transmission travel time through propagating medium can be recorded by GPR data acquisition storage system and the depth of buried pipe, D , can be estimated using Equation 2 [10];

$$D = \frac{Tv}{2} \quad (2)$$

where T is the travel time of the transmitted and reflected wave in nanoseconds and v is the wave velocity. The strength of the electromagnetic reflection is proportional to the magnitude of the dielectric property in contrast with the amount of energy reflected being given by the reflection coefficient, R , expressed as:

$$R = \frac{\sqrt{v_1} - \sqrt{v_2}}{\sqrt{v_1} + \sqrt{v_2}} \quad (3)$$

where v_1 and v_2 are the wave velocities of pipe and soil, respectively [11]. Generally, the values of reflection coefficient range between -1 and +1, with values further from 0 representing greater differences in dielectric properties. Therefore, the difference in measured pipe depth (Equation 2) when the GPR wave travels through dry soil and saturated soil can be used to denote the leakage state of buried pipes.

Therefore, in this study, the detection of the leakage of buried pipes is by interpretation based on the change in pipe depth measurement, D [12], and the existence of hyperbolic feature as the GPR wave travels through the soils with different saturation conditions.

2. Methodology

2.1 Experimental setup

A prototype model was set up as shown in Figure 1. It consists of a plastic box and a plywood cover which is placed on top of the box and acts as a bridge allowing GPR to be moved above the plastic box. The plastic box dimensions are 61 cm long, 31 cm high and 42 cm wide. First, the plastic box is filled up with dry sand as a medium of pipe embedment; while later, in the second stage, it is filled up with dry soil as the medium. Two PVC pipes are then placed and buried in the sand at a depth of 24 and 23 cm from the top of the soil. Holes were introduced at the middle of the pipes by drilling the pipes and water leakage condition is simulated by injecting water at four different stages.

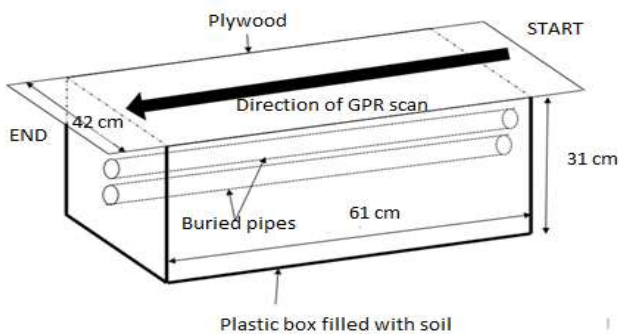


Fig. 1: Schematic diagram of the prototype model

2.2 Pipe leakages simulation and GPR data collection for leakage state detection

In order to simulate pipe leakages condition, first, 1000 mL quantity of water was supplied into the PVC pipes consecutively; i.e. 500 mL water at time 0 second and another 500 mL water after the next 20 seconds. The water was subsequently drained out through the holes located at the middle of the buried pipes. Four numbers of B-scan GPR data were captured in order to characterize the empty pipe state and pipe leakages state.

The initial 1.6 GHz centre frequency GPR B-scan was conducted over empty PVC pipes before the first 500 mL water was supplied into the pipes (as shown as Profile A after analysis). This serves as the reference empty pipe state of GPR data. As the first 500 mL water was supplied in the system, B-scan GPR data were collected on the embedded pipes after 5 seconds (as shown as Profile B after analysis). After 20 seconds, another 500 mL water was injected into the pipes and GPR antennae were used to scan the B-scan data in this state (as shown as Profile C after analysis). The final GPR scanning process were repeated over the pipes after 60 seconds to observe the final state of the water leakages (as shown as Profile D after analysis).

2.3 GPR image analysis and interpretations

The GPR wave signals were then analysed using RADAN 6.6 software to obtain the images of the embedded pipes in different soils under two conditions; without and with the water injection, to study the effect of water leakages in pipes embedded in the soil. B-scan data were stored in the internal storage unit in the GPR system. The computation of the wave velocity analysis on each soils was done by using the

migration analysis tools in RADAN software. Parameters such as GPR wave travel time, T , and its wave velocities, v , also were computed automatically using migration analysis for each profile by RADAN 6.6 software. Migration analysis technique was used to find the dielectric constant of the soils using RADAN by solving the wave propagation equation in the frequency wave domain. The wave velocity, v , is computed using Equation (1) based on the dielectric constant determined by the migration analysis.

3. Results and discussions

3.1 The effect of pipe leakages on GPR wave reflection signals

Four different GPR signal profiles of B-scan data were collected during the experiments, i.e. before, during and after injection of the water through the embedded pipe in the soils. The typical results of the GPR signals on four profiles are shown in Figure 2 to Figure 5 and summarized in Table 1.

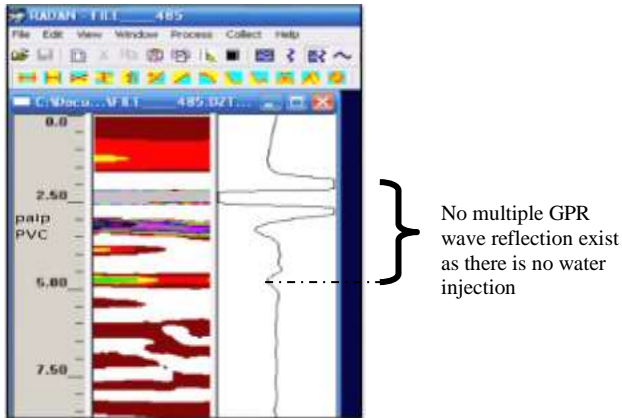


Fig. 2: GPR signal before the water addition (Profile A)

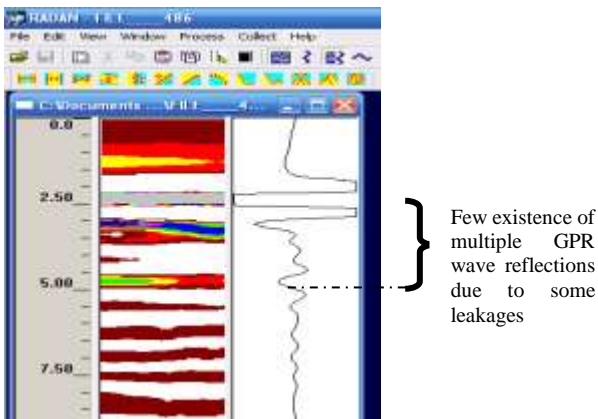


Fig. 3: GPR signal Profile B

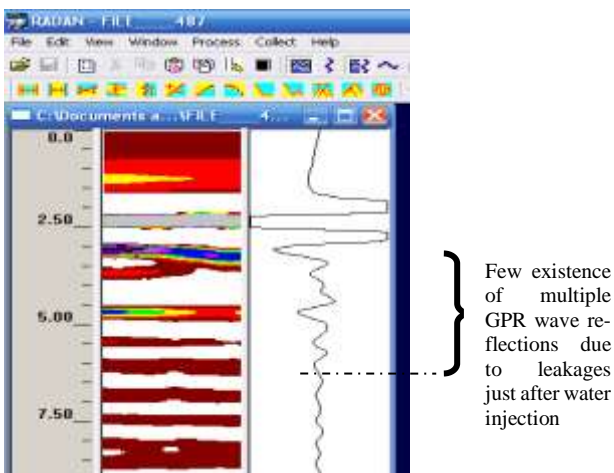


Fig. 4: GPR signal Profile C

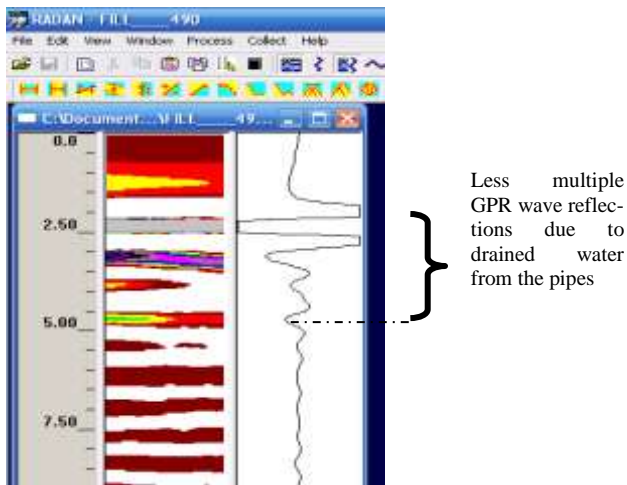


Fig. 5: GPR signal Profile D

Table 1: Average pipe depth results of each profile

Profile	Time travel, T (ns)		Depth of pipes (m)		Difference between the estimated and actual depth (%)	
	Sand	Dry soil	Sand	Dry soil	Sand	Dry soil
A	2.79	2.92	0.2416	0.219	0.99	1.05
B	2.80	2.95	0.2420	0.221	1.01	1.04
C	2.93	2.96	0.2314	0.215	1.04	1.07
D	2.94	2.98	0.2322	0.216	1.03	1.07

It can be seen that there is no existence of multiple wave reflection in the empty pipe at time $t = 0$ second as shown in Figure 2. However, when the first 500 mL water is injected into the embedded pipes, few GPR multiple wave reflections were observed in the Profile B and C (Figure 3 and 4) as the water flows in the pipes. The multiple wave reflections occurred due to GPR wave refraction as the wave hit the 500 mL water surface and attenuated the wave energy by both scattering and absorption mechanism [13-14]. However, as the water is being drained out through the hole, less multiple GPR waves reflection were observed, denoting lesser wave energy attenuation due to the few absorption and scattering on GPR waves as shown in Figure 5.

The pipe leakages in the soil can also be recognized by the change of the piped depth, D , i.e. the reduction of the computed embedded pipe depth and by the increased value of time travel (T) before and after the water was injected for both sandy soil and dry soil. As given in Table 1, when the water is injected at 20 s and 60 s through the pipes, the computed embedded pipe depths were varying from the real depth by 0.99 to 1.04 percent (sandy soil) and from 1.05 to 1.07 percent (soil). The varying embedded pipe depths condition is primarily explained by the increased in dielectric constant of the sandy soil due to water injection at 5 s and 20 s. Also, it can be seen that, sand loses moisture quicker than dry soil, by observing the time travel of the waves.

3.2 The effect of leakages on hyperbolic shape, GPR time travel, GPR wave velocity and soil dielectric constant value

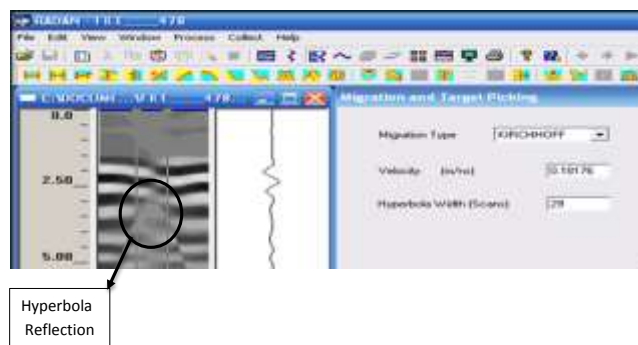


Fig. 6: Hyperbolic shape Profile A (sand)



Fig. 7: Hyperbolic shape Profile B (sand)

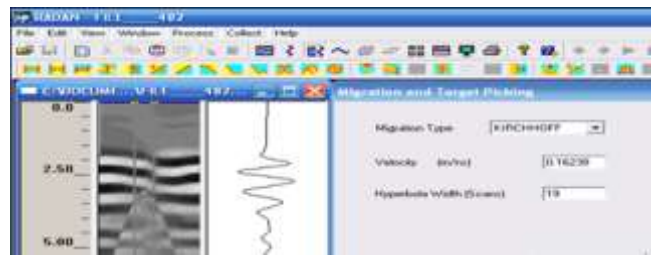


Fig. 8: Hyperbolic shape Profile C (sand)

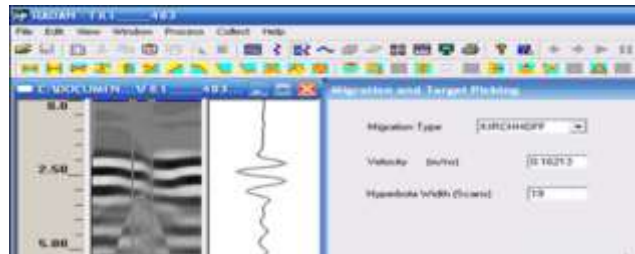


Fig. 9: Hyperbolic shape Profile D (sand)

Figure 6-9 shows the hyperbolic shape of the reflected wave for the buried pipes. Referring to these figures and Table 2, when there is no water injected through the pipe (Profile A), the width of the hyperbolic shape of reflected wave on the pipe is the widest compared to the other profiles. The velocity of Profile A is the highest numerical values as the GPR waves travel faster in air (empty pipes). As the water is injected, the width of the hyperbola is reduced, i.e. up to stage D, the width of the hyperbola is reduced from 29 to 19.

It can be observed that the wave velocity of sand medium from profile A as shown in Table 2 is the highest compared to others. This condition can be explained by changing the dielectric constant value of the dry sand state to saturated sand condition. The computed dielectric values of the dry sand (3.39) agrees with the dielectric constant range values given by [15]. The changing geometry/shape/width of hyperbola denotes the location of the pipe leakages in soil, as mentioned by [6].

As the water is being injected into the sand, the wave velocity is decreased from 0.1818 m/ns to 0.1621 m/ns as the soil dielectric constant is increased from 3.39 to 4.57, which agrees with the dielectric values given by reference [16]. The increment of water content in any medium attenuates the GPR wave reflection signal [17]. The decreased of the wave velocity and the increased of dielectric constant prove that the existence of water leakages in the sand. Similar pattern is also depicted by the data presented for dry loose soil.

Table 2: Average hyperbola width and calculated velocity and dielectric constant of each profile

Profile	Hyperbola width		Velocity (m/ns)		Dielectric constant	
	Sand	Dry soil	Sand	Dry soil	Sand	Dry soil
A	29	29	0.1818	0.1628	3.39	3.39
B	27	21	0.1732	0.1585	3.58	3.58
C	19	21	0.1624	0.1447	4.30	4.30
D	19	19	0.1621	0.1404	4.57	4.56

4. Summary and conclusions

GPR has been employed in this study and served as a tool for detecting water leakages and location of embedded pipes in soils. It was observed that water plays the most important factors influencing the GPR wave velocity and dielectric constant of the embedded soil surrounding the pipes. The appearance of the hyperbola features is delayed and the reflection is attenuated when water content increases. Most leakages are detectable by observing radar signal velocity reduction and dielectric constant increment due to the increment of the water content in the soil. However, these results are limited only to uncontaminated and shallow depth soil medium (less than 0.5 m). High concentration salt and ferric in certain soil will substantially scattered the incoming GPR wave before being reflected to the receiver antenna. The presence of natural ground water table will also create false alarm result on the water leaks problem.

Acknowledgement

The authors acknowledged Universiti Kebangsaan Malaysia for their financial support via the allocation grant under project DIP-2014-019.

References

- [1] Hyun SY, Jo YS, Oh HC & Kim SY (2003), An experimental study on a Ground Penetrating Radar for detecting water-leaks in buried water transfer pipes, *International Symposium on Antennas, Propagation and EM Theory (ISAPE)*, 596-599.
- [2] Berita Harian, available online: <http://www.bharian.com.my/node/90337>, 20 October 2015. Accessed May 19, 2018.
- [3] Eyuboglu S, Mahdi H & Shukri AH (2003), Detection of water leaks using ground penetrating radar, *Geophysics 2003: Conference on Applied Geophysics*, 8-12.
- [4] Hunaidi O & Giamou P (1998), Ground-penetrating radar for detection of leaks in buried plastic water distribution pipes, *Proc. of the 7th International Conference on Ground Penetrating Radar*, 783-786.
- [5] Stampolidis A, Soupios P & Vallianatos F (2003), Detection of leaks in buried plastic water distribution pipes in urban places – A case study, *2nd International Workshop on Advanced GPR*, 120-124.

- [6] David AC, Manuel H, Joaquin I, Silvia JOL & Rafael PG (2013), GPR-based waterleak model in water distribution systems, *Sensors* 2013 , Vol.13, No. 12, 15912-15936, available online: <https://doi.org/10.3390/s131215912>.
- [7] Daniels DJ, *Ground Penetrating Radar Fundamentals, Institution of Engineering and Technology, 2nd Edition*, Stevenage: Institution of Engineering and Technology, (2007).
- [8] Sbartai JM, Laurens S, Balayssac JP, Ballyy G & Arliguie G (2006), Effect of concrete moisture on radar signal amplitude, *ACI Materials Journal*, Vol. 103, No. 6,419-426, available online: <https://doi.org/10.14359/18219>.
- [9] Chiflar J & Ulaby FT (1974), Dielectric properties of soils as a function of moisture content, National Aeronautics and Space Administratio, Texas, RSL Technical Report 177-47, 68.
- [10] Bungey JH (2004), Sub-surface testing of concrete: a review, *Construction and Building Materials*, Vol. 18, No. 1, 1-8, available online: [https://doi.org/10.1016/S0950-0618\(03\)00093-X](https://doi.org/10.1016/S0950-0618(03)00093-X).
- [11] Neal A (2004), Ground-penetrating radar and its use in sedimentology: principles, problems and progress, *Earth science reviews*, Vol. 66, No. 3-4, 261-330.
- [12] Abouhamad M, Zayed T & Mohelsi O (2016), leak detection in buried pipes using ground penetrating radar – a comparative study, *Proc. Of the Pipelines* 2016, 417, available online: <https://doi.org/10/1061/9780784479957.039>.
- [13] Saharudin MA, Nordiana MM, Nordiana AN & Maslinda U (2016), Application of ground penetrating radar (GPR) in detecting target of interest, *International Research Journal on Engineering and Technology*, Vol. 3, No.1, 48-53.
- [14] Grimm RE, Heggy E, Clifford S, Dinwiddie C, McGinnis R & Fareell D, (2006), Absorption and scattering in ground-penetrating radar: Analysis of Bishop Tuff, *Journal of Geophysical Research*, Vol. 111, 1-15.
- [15] Daniels DJ (1996), Surface-penetrating radar—IEE Radar, Sonar, Navigation and Avionics Series, *The Institute of Electrical Engineers London*, 5, 357-361.
- [16] Reppert PM, Morgan FD & Toksov MN (2000), Dielectric constant determination using ground-penetrating radar reflection coefficients, *Journal of Applied Physics* 43, 189-197.
- [17] Senin SF & Hamid R (2016), Ground penetrating radar wave attenuation models for estimation of moisture and chloride content in concrete slab, *Construction and Building Materials*, Vol. 106 , 659-669, available online: <https://doi.org/10.1016/j.conbuildmat.2015.12.156>.